JOURNAL OF SPACECRAFT AND ROCKETS
Vol. 44, No. 5, September–October 2007

End-to-End Analysis of Solar-Electric-Propulsion Earth Orbit Raising for Interplanetary Missions

Grant Bonin* and Tarik Kaya†
Carleton University, Ottawa, Ontario K1S 5B6, Canada

DOI: 10.2514/1.28670

An end-to-end investigation of solar electric Earth orbit raising for interplanetary missions is discussed. In such mission designs, a solar electric tug is used to elevate an interplanetary payload from an initial low-Earth orbit to a highly eccentric Earth orbit, after which the tug is released and interplanetary injection is performed by a small chemical upper stage. Launching payloads from highly eccentric orbits allows for a dramatic reduction in the velocity change required for interplanetary missions, as contrasted against direct injection from the Earth's surface or low-Earth orbit. Correspondingly, significantly higher payload mass fractions can be achieved using solar electric Earth-orbit-raising mission designs. However, although highly promising as a potential means of dispatching interplanetary payloads, a number of key factors are identified that can severely limit such potential. In particular, propellant boil-off in the chemical upper stage during orbit raising can lead to payload-optimal specific impulse values in many cases. Additional considerations such as the desirability of solar electric tug reuse can further contribute to marginalize the benefits of solar electric Earth orbit raising with respect to competing propulsion options. This study investigates key issues associated with solar electric Earth-orbit-raising missions, including circumstances leading to payload-optimal specific impulse values, payload-optimal inclinations for orbit raising, and achievable relative payload gain rates for solar electric Earth-orbit-raising missions compared with all-chemical injection scenarios. A new variation of the low-thrust rocket equation is derived for interplanetary missions. Finally, a novel form of orbital transfer, referred to as an Earth-eclipse-evading transfer, is also introduced, which can potentially increase achievable solar electric Earth-orbit-raising payload ratios and rates when higher-inclination orbits are accessible. It is concluded that solar electric Earth orbit raising represents a promising way of undertaking interplanetary missions, but that constraints nevertheless exist that can powerfully reduce the effectiveness of such mission designs.

Nomenclature

a	=	semimajor axis, km
C_3	=	launch energy, km^2/s^2
c	=	exhaust velocity, m/s
E	=	eccentric anomaly, rad
e	=	eccentricity
F	=	eccentric longitude, rad
f	=	spacecraft component fraction
i	=	inclination, deg
m	=	spacecraft mass, kg
P	=	spacecraft power, kW
PR	=	payload ratio
r_A	=	apogee radius, km
r_P	=	perigee radius, km
T	=	thrust, N
TOF	=	time of flight, days
$\hat{\boldsymbol{u}}$	=	unit vector
$\boldsymbol{x}$	=	equinoctial state vector
Δv	=	velocity change, m/s
δ	=	relative payload gain rate, days^{-1}
ε	=	velocity elasticity
η	=	thrust efficiency
κ	=	propellant boil-off rate, kg/month
λ	=	propellant loss ratio
μ	=	earth gravitational parameter, km^3/s^2
ν	=	true anomaly, rad
ρ	=	specific power mass, kg/kW
Ω	=	right ascension of ascending node, rad
ω	=	argument of perigee, rad

Received 1 November 2006; revision received 22 February 2007; accepted for publication 1 March 2007.

*Research Assistant, Department of Mechanical and Aerospace Engineering, 1125 Colonel By Drive; gbonin@connect.carleton.ca.

†Associate Professor, Department of Mechanical and Aerospace Engineering, 1125 Colonel By Drive; tkaya@mae.carleton.ca.

I. Introduction

DEPARTURE from the Earth's gravitational sphere of influence is one of the greatest difficulties associated with interplanetary flight. Indeed, for even relatively low-energy launch opportunities for destinations such as Mars, greater than 80% of the total propulsive velocity change is required for Earth escape alone. This, in turn, generally requires that a significant initial mass be launched from Earth's surface to dispatch any substantial payload onto an interplanetary transfer when exclusively chemical propulsion systems are used.

However, although the preceding statement applies ubiquitously for even the most energy-efficient rocket stages, a potentially promising alternative to an entirely chemical propulsion system for such missions would be the use of solar electric (SE) propulsion. Although incapable of performing direct interplanetary injection maneuvers and potentially problematic for extended use in interplanetary space, significant promise nevertheless exists in the compromise approach of using SE systems for initial Earth orbit raising. In such scenarios, a solar electric tug is used to elevate an interplanetary spacecraft from an initial position in low-Earth orbit (LEO) to a highly eccentric Earth orbit (HEEO), after which the SE tug would be detached from the payload and a small chemical stage would be used to complete the interplanetary injection maneuver. Dividing the propulsion required for interplanetary injection between low- and high-thrust propulsion systems allows the preponderance of the velocity change required for Earth departure to be executed by a higher-efficiency continuous-low-thrust system over the course of several months. Then, the final injection is performed by an impulsive maneuver from a high-thrust engine at perigee, thus maximizing the benefits of injection from HEEO. This compromise approach of SE-based Earth orbit raising followed by chemical injection holds significant promise for reducing the initial mass in low-Earth orbit (IMLEO) required to support a given mission.

This study performs an end-to-end analysis of the potential of solar electric Earth orbit raising (SE-EOR) for interplanetary missions. What is meant by end to end is that all mission and spacecraft design phases and characteristics are considered at the systems level, and the sensitivity of SE-EOR to variations in key parameters is analyzed at all stages in the orbit-raising process. Although end-to-end analysis has been used in past studies to include the launch phase [1], for the purposes of this study, mission considerations begin in LEO. In particular, the impact of required interplanetary launch energy C_3 and propellant boil-off in the cryogenic upper stage used for interplanetary injection are addressed and coupled to overall system performance in both numerical and analytical analyses. The conclusions derived from this study can serve as both a tool for early systems-level analysis of SE-EOR in interplanetary missions, as well as cautionary observations to be noted early in propulsion design and selection.

II. Background and Motivation

The concept of using a continuous-low-thrust SE propulsion system to transfer an interplanetary payload from LEO to HEEO is not a novel one and has been investigated at length by teams at NASA's Johnson Space Center and John H. Glenn Research Center [2,3] as an addendum to NASA's Human Mars Design Reference Mission (DRM) 3.0 [4]. The DRM addendum represented a departure from previous NASA studies of human Mars missions, which had generally been predicated on the use of nuclear thermal propulsion for the entire trans-Mars injection maneuver. Presumably, the switch to SE propulsion was due to political concerns with the development and deployment of large-scale space-based nuclear reactors, as well as the uncertainty in redeveloping nuclear thermal rocket technology. In the proposed NASA mission, an SE tug would be used to raise large Mars-bound payloads from an initial 51.6-deg-inclination, 400-km circular LEO to an 800 by 65,000-km HEEO, after which a cryogenic upper stage would be used for trans-Mars injection. The tug would subsequently be returned to LEO for reuse. The entire orbit-raise flight time would be on the order of 6–12 months, depending on the power/mass ratio of the SE tug.

However, further documentation on the NASA SE-EOR investigation beyond the preceding cited references is sparse, and the viability of SE-EOR does not appear to have been further investigated elsewhere in literature. Although Oh et al. [1] developed linearized analytical models for SE-EOR between elliptical and geostationary orbit (GEO) for commercial applications, such models are not particularly applicable to the analysis of mission designs in which SE propellant mass grows large with respect to overall spacecraft mass. Furthermore, in addition to the limited information available for mission planners on SE-EOR, those few published examinations have been somewhat limited in scope. Only large human-class payloads appear to have been analyzed, and the impact of either upper-stage propellant boil-off or varying interplanetary launch energies does not appear to have been considered. Furthermore, the requirement in such human-class missions that the SE tug be reused for multiple orbit raises can further act to marginalize the potential benefits of such systems, because approximately 25% of the total SE propellant mass must be held in reserve for a return flight to LEO. In the context of this concern, as well as that of reduced available power from radiation-degraded solar power systems after slow spiraling through the Van Allen belts during the initial orbit raise, the trade space between a large tug, its reuse, and competing propulsion options does not appear to have been thoroughly considered in previous works.

Although benefits certainly appear to exist in SE-EOR for some mission designs, it seems that no comprehensive analysis of SE-EOR has yet been published in open literature that couples the preceding considerations in attempting to ascertain its viability for interplanetary missions. This paper represents the first attempt to fully consider the sensitivity of interplanetary SE-EOR mission designs to the aforementioned effects, as well as others noted in later sections, such that the trade space for SE-EOR can be fully understood by planners of both large and small missions. To accomplish this comparison, a direct optimization code is validated for the first time in literature for transfers to orbits with extremely high terminal eccentricities, and algorithms are presented for postprocessing and evaluating the performance of SE-EOR mission designs following continuous-low-thrust trajectory optimization. A novel form of SE transfer and a new variation on the low-thrust rocket equation are also introduced.

III. Methodology

In this section, we define and discuss the key figures of merit used in this study, upon which the majority of analyses performed herein are based. In particular, payload ratio and relative payload gain rate are identified as major SE-EOR performance standards. A new method of characterizing the relative benefits of SE-EOR, referred to as velocity elasticity, is also introduced.

A. Performance Standards and Key Metrics

1. *Payload Ratio and Relative Payload Gain Rate*

The principal goal of this study was to determine the combination of SE-EOR and chemical injection that maximizes the ratio of total payload to initial mass in LEO, defined as a mission's payload ratio (PR). Because of the coupling of several systems-level factors, the maximum achievable payload ratio in SE-EOR interplanetary missions is not necessarily achieved by combining the highest possible performance SE and chemical propulsion systems, as might otherwise be expected when considering the two propulsion options independently.

Although payload ratio is generally regarded as the variable of greatest importance in space mission design, it is noted that mission time also has an inherent value that must also be considered, particularly as a strong driver of mission operations cost. For this reason, SE trajectories in this study are optimized for minimum time, as opposed to minimum fuel. Minimum fuel transfers almost always necessitate longer flight times, except in the circumstance in which SE fuel mass flow rate is constant, and the minimum fuel solution is the same as the minimum time solution.

To quantify the relative gains achievable in SE-EOR mission designs per unit time, we define a quantity, the relative payload gain rate, as

$$\delta = 100 \times \frac{(PR_{\mathrm{SE}} - PR_{\mathrm{chem}})/PR_{\mathrm{chem}}}{TOF_{\mathrm{SE}} - TOF_{\mathrm{chem}}} \tag{1}$$

which is simply the percent difference in payload ratios between SE and chemical injection systems, divided by the difference in flight time between each scenario. Because in general $TOF_{\mathrm{chem}} \ll TOF_{\mathrm{SE}}$, we make the approximation

$$\delta \cong 100 \times \frac{(PR_{\mathrm{SE}} - PR_{\mathrm{chem}})}{PR_{\mathrm{chem}} TOF_{\mathrm{SE}}} \tag{2}$$

The relative payload gain rate is a particularly telling metric, providing mission planners with a sense of the achievable gain in mission payload ratio per unit time of operation. This can in turn be used in mission cost analysis, in which operations time is often traded against the relative benefit of increased-duration SE use.

2. *C_3 and Velocity Elasticity*

A key metric that is generally used to characterize an interplanetary launch opportunity is the specific launch energy C_3 required for Earth departure. C_3 is simply the square of the hyperbolic velocity (also referred to as departure velocity) required to accomplish a given transfer. In turn, the departure velocity is the vector difference of the heliocentric velocity required for a given injection and the characteristic velocity of the Earth around the sun.

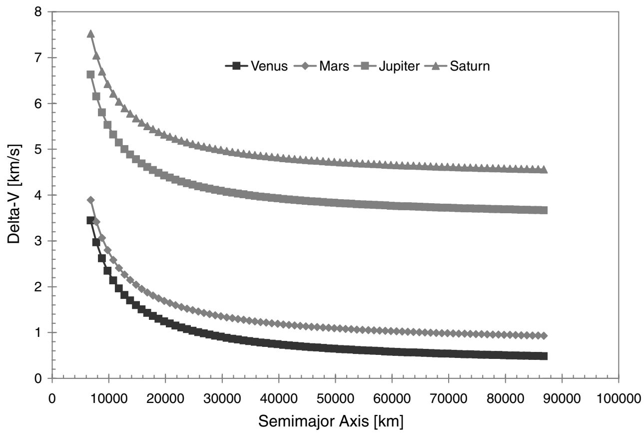

Fig. 1 Interplanetary Δv as a function of the Earth semimajor axis for candidate destinations.

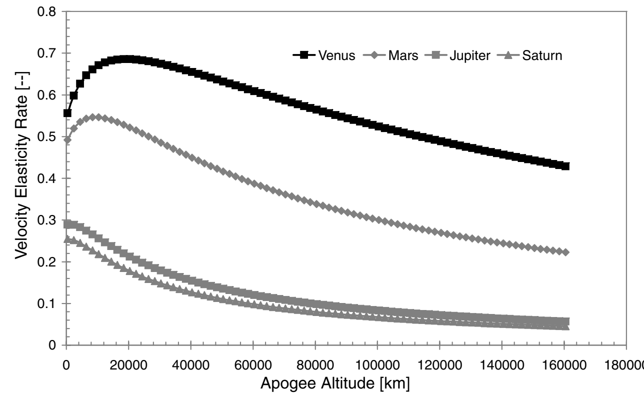

Fig. 2 Velocity elasticity rate vs apogee altitude for varying interplanetary targets.

For minimum-energy transfers to Mars, C_3 can range between approximately 9 and 16 $\mathrm{km}^2/\mathrm{s}^2$, depending on the launch opportunity in question. For outer planetary destinations such as Jupiter and Saturn, it is much higher, ranging between 87 and 113 $\mathrm{km}^2/\mathrm{s}^2$ for the two largest planets, respectively, when planetary gravity assists are not employed.

Although C_3 is fixed by the characteristics of the desired interplanetary trajectory, the total velocity change required to perform the transfer from Earth is not. The principle behind SE-EOR is that the ratio of mass launched into orbit to support an interplanetary mission (including propellant, tanks, engines, power systems, etc.) to the mass of payload can be minimized by amortizing the propulsive requirements for a given mission over a combined long-duration, continuous-low-thrust, orbit-raising phase followed by an impulsive chemical-based Earth-escape maneuver.

The impulsive velocity change Δv is the component that is theoretically desirable to minimize, because it must come from a high-thrust, relatively inefficient, engine. Figure 1 shows the chemical Δv needed for minimum-energy flights to the aforementioned candidate destinations as a function of the final semimajor axis achieved by the solar electric orbit raise. Each final orbit in Fig. 1 is assumed to have a perigee of 400-km altitude.

Although Fig. 1 shows that the required impulsive Δv falls off exponentially with increasing SE-EOR altitude, it is also apparent that the lion's share of Δv reduction can be achieved for semimajor axes below 20,000 km. This is advantageous in terms of time economy, because SE-EOR is an extremely slow process, requiring long spiral trajectories and repeated passages through the Van Allen radiation belts. To quantify the percent velocity change reduction associated with percent increases in altitude, we define ε, the velocity elasticity, as

$$\varepsilon = \frac{\partial \Delta v}{\partial a}\frac{a}{\Delta v} \tag{3}$$

where a is the semimajor axis of the final Earth orbit attained by the electric-driven orbit raise. Velocity elasticity represents a measure of the percent reduction in required impulsive velocity change with respect to percent increases in the semimajor axis. From a given interplanetary mission characterized by its C_3, and with chemical injection performed from a perigee radius r_P, the velocity elasticity can be calculated as

$$\varepsilon = \frac{r_A \mu}{\sqrt{2}\Delta v}\left[\sqrt{\mu\left(\frac{1}{r_P} - \frac{1}{r_P + r_A}\right)}(r_P + r_A)^2\right]^{-1} \tag{4}$$

where r_A is the apogee radius of the final HEEO and μ is the Earth's gravitational parameter. Note that, as is apparent from Fig. 1, the partial derivative $\partial\Delta v/\partial a$ is independent of the C_3 required for a given interplanetary transfer, though ε itself is not. By differentiating the velocity elasticity, setting to zero, and solving for r_A, we can find the target apogee radius above which velocity change reductions scale increasingly slowly per unit of altitude increase. Figure 2 shows the rate of change of velocity elasticity with respect to altitude versus increasing target apogee for candidate destination planets. For minimum-energy flights to Mars, this "elastic altitude" is approximately 8500 km, which is far lower than intuition might otherwise suggest. For destinations such as Jupiter and Saturn, the rate of velocity change reduction with respect to altitude gain is found to increasingly diminish for all altitudes.

B. Computational Methods

The most widely used computational method for time-minimized continuous-low-thrust trajectory optimization is NASA's Solar Electric Propulsion Steering Program for Optimal Trajectory (SEPSPOT) [5,6][‡]. Originally developed in the early 1970s as the Solar Electric Control Knob Setting Program for Optimal Trajectories (SECKSPOT), SEPSPOT uses a shooting method and a calculus of variations approach to solve the two-point boundary-value problem (2PBVP) formulated by user-specified initial and final (target) spacecraft orbits. This and similar approaches using calculus of variations are generally referred to as indirect methods. In SEPSPOT, first-order conditions for trajectory optimality are derived from initial user-defined guesses as to a vector of augmented performance indices (equinoctial costate or adjoint variables), and the time-averaged histories of the costates are used to define an optimal steering and thrust profile for the transfer. However, SEPSPOT is known for its extreme sensitivity to the initial costate vector guess, which may not be intuitive for even experienced users to make. Furthermore, convergence in SEPSPOT becomes difficult to achieve when one or more of the program's environmental models (radiation-induced power degradation, Earth shadowing, or Earth oblateness) are initialized or for orbits with eccentricities larger than 0.75. The extreme sensitivity of SEPSPOT to these factors makes solution of the 2PBVP both difficult and uncertain. Finally, the requirement for a newly formulated 2PBVP with each target orbit raise in SEPSPOT makes any in-depth analysis of SE-EOR challenging and time-consuming. However, although depending to great extent on the quality of the initial costate guess, the advantage of indirect methods such as SEPSPOT is that when a solution is obtained, it is almost always the optimal solution.

Although SEPSPOT was used in the initial stages of this study, its limitations were quickly realized, and a solar-electric-propulsion direct optimization code (SEPDOC) was subsequently employed for trajectory analysis [7]. Contrary to SEPSPOT, the direct optimization code replaces the optimal control problem of indirect methods with a nonlinear programming problem, which is developed by parameterizing the states or controls by a finite number of optimization parameters. These parameters are subsequently adjusted by an optimization method that attempts to directly reduce

[‡]Data available online at http://trajectory.grc.nasa.gov/tools/sepspot.shtml [retrieved 3 June 2006].

an overall performance index with each iteration. The advantage of direct methods is that the 2PBVP becomes simple and intuitive for a user to formulate and solve, making it much easier to generate an initial guess in the region of the optimum solution. The direct optimization code thus exhibits far more robust convergence properties than SEPSPOT. The disadvantages of direct methods are that computation time is greatly increased and there is susceptibility to the program converging to local minimums.

Typically, a gradient method is used to search the design space for a set of optimal design parameters in direct optimization. The direct method employed in this study uses a set of weighted optimal control laws to parameterize the continuous-thrust direction angles, and the control laws themselves are parameterized by linear interpolation, with the interpolation points treated as optimization variables. The direct method employed in this study uses sequential quadratic programming (SQP) to solve the nonlinear programming problem. The SQP code used by SEPDOC is NPSOL [8], which uses finite differences to compute missing gradient information not provided by analytic equations.

1. Equations of Motion

Because most SE transfers require extremely long flight times to complete, orbital averaging is used for the governing dynamics of spacecraft motion. Earth shadow and solar cell degradation due to passage through the Van Allen radiation belts are also considered.

For the continuous-low-thrust transfer problem, a maximum of seven state variables are used: five slowly varying modified equinoctial elements, spacecraft mass, and equivalent 1-MeV fluence for solar cell radiation degradation. For cases in which power degradation is not considered, the problem therefore only has six states.

The general equation for orbital averaging can be written as

$$\frac{\mathrm{d}\bar{\mathbf{x}}}{\mathrm{d}t} = \frac{1}{T}\int_{F_{\mathrm{ex}}}^{F_{\mathrm{en}}} \frac{\mathrm{d}\mathbf{x}}{\mathrm{d}t}\frac{\mathrm{d}t}{\mathrm{d}F}\,\mathrm{d}F \tag{5}$$

where $\boldsymbol{x} = [a \;\; h \;\; k \;\; p \;\; q \;\; m]^T$ is the 6×1 state vector containing the five equinoctial orbital elements and spacecraft mass m. The preceding modified equinoctial orbital elements are related to the classical orbital elements $[a \;\; e \;\; w \;\; \Omega \;\; i \;\; \nu]^T$ by the following equations:

$$h = e\sin(\omega + \Omega) \tag{6}$$

$$k = e\cos(\omega + \Omega) \tag{7}$$

$$p = \tan(i/2)\sin\Omega \tag{8}$$

$$q = \tan(i/2)\cos\Omega \tag{9}$$

$$F = \Omega + \omega + E \tag{10}$$

where

$$E = \arccos\left(\frac{e + \cos\nu}{1 + e\cos\nu}\right) \tag{11}$$

is the eccentric anomaly and F is referred to as the eccentric longitude, which is a broken-plane angle from the inertial x axis to the spacecraft, as measured in the equatorial and orbital planes. Of the above five modified elements, F is the only one that varies quickly. All others are chosen as slowly changing variables for the sake of using orbital averaging.

The orbital-averaging technique computes the mean rate of change $(\mathrm{d}\bar{\boldsymbol{x}}/\mathrm{d}t)$ of a slowly changing orbital element by dividing the incremental change of an orbital element per revolution by the period of that revolution. The integral in the orbital-averaging equation is the incremental change in the orbital element per revolution and T is the period. All five slowly varying orbital elements are held constant during evaluation of the integral. The equinoctial element state vector rate of change is computed as

$$\frac{\mathrm{d}\boldsymbol{x}}{\mathrm{d}t} = a_T \mathbf{M}\hat{\boldsymbol{u}} \tag{12}$$

where $\mathbf{M}$ is a 5×3 matrix, a_T is the magnitude of the SE thrust acceleration, and $\hat{\boldsymbol{u}}$ is a unit vector in the thrust direction in either the modified or classical equinoctial frame. Matrix $\mathbf{M}$ is a function of the six equinoctial elements, for which the individual entries are presented in detail by Kluever and Oleson [7]. The inverse time rate for F is

$$\frac{\mathrm{d}t}{\mathrm{d}F} = \frac{1 - k\cos F - h\sin F}{2\pi} \tag{13}$$

and the shadow exit and entrance angles are the limits of the orbital-averaging integration. When shadowing effects are not included, the integration limits are simply 0 and 2π. When radiation effects are included, a seventh state variable is included for the flux factor and the integration limits are always 0 and 2π. A tabular method is used for determining the degraded solar array power during a given trajectory [7]. The orbital-averaging integral is evaluated numerically using the eight-point Gaussian quadrature method from SEPSPOT, and the averaged dynamical equations are numerically time-integrated using a fixed-step fourth-order Runge–Kutta with user-defined step sizes. A single Euler integration step is used to compute the final orbital state. A detailed description of the optimal control law used in SEPDOC can be found in [7,8].

The direct method treats the thrust-to-power ratio of the SE propulsion system as a function of the system's exhaust velocity c:

$$\eta \equiv \frac{1}{P}\left(\frac{1}{2}\dot{m}c^2\right) \tag{14}$$

and because $T = \dot{m}c$, we can write

$$\frac{T}{P} = \frac{2\eta}{c} \tag{15}$$

which is a frequently used sizing equation [9] that couples power supply mass penalties to increased engine thrust efficiency. Gillard's efficiency equation [1] is used to relate the thrust efficiency to specific impulse as

$$\eta = \frac{bc^2}{c^2 + d^2} \tag{16}$$

where $c = gI_{\mathrm{sp}}$, and b and d are thruster specific constants. An SPT-140 engine in this analysis is used to represent a typical Hall thruster, and Hall constants are taken from [1]. A fit for a derated ion thruster is taken from Oleson [10]. The constants used are presented in Table 1.

2. Validation of the Direct Method

The direct optimization code employed in this study has been validated for both LEO to GEO and geostationary transfer orbit (GTO) to GEO transfers in the past [7]. However, no validation of the direct method has yet been published demonstrating its potential for optimizing trajectories with very large terminal eccentricities (greater than 0.7). This is a problem to which the direct code was

Table 1 Thruster efficiency curve-fitting constants

Thruster	b	d, m/s
SPT-140	0.684	7,998
Ion thruster	0.825	14,570

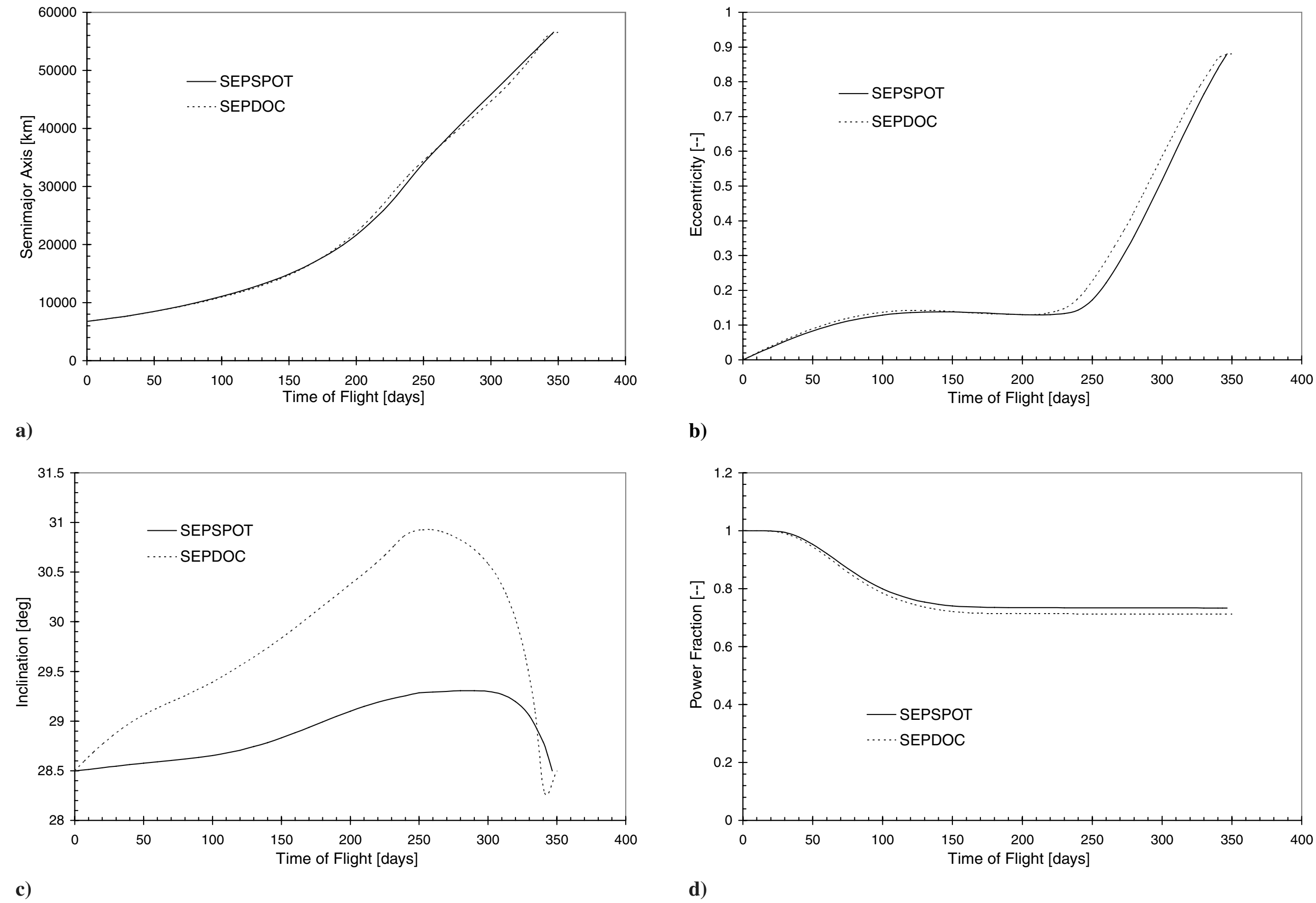

Fig. 3 Comparison of SEPSPOT and SEPDOC program outputs for semimajor axis, eccentricity, inclination, and power fraction histories as a function of time of flight.

found to be very sensitive, particularly with shadowing effects accounted for, which tend to drive a negative eccentricity rate.

However, once large initial costate weighting functions for eccentricity were chosen to produce positive $\mathrm{d}e/\mathrm{d}t$ steering, convergence in the direct method was found to be very robust, with results that closely match those obtained with SEPSPOT. Figure 3 shows the time histories of the classical equinoctial orbital elements and spacecraft power fraction for a coplanar transfer from an initial 28.5-deg, 400-km circular LEO to a 400 by 80,000-km HEEO (a particularly difficult case to converge). The specific impulse of the spacecraft is taken as 2200 s, $\eta = 0.601$, and a specific power of 5 W/kg. Both Earth shadowing and radiation-induced power degradation are assumed. Oblateness effects are not considered.

Although the direct method is expected to lose accuracy near the end of a transfer to a high-energy orbit, Fig. 3 nevertheless demonstrates the capabilities of the direct optimization code. Although there are slight discrepancies in the inclination histories of the direct method when compared with SEPSPOT, it is hypothesized that the direct optimization code increases inclination as a means of avoiding radiation degradation, because passage through the Van Allen radiation belts is less detrimental at higher inclinations. However, because the final power ratio calculated by the direct code is slightly less than the SEPSPOT result, the slight inclination discrepancy may simply be an artefact of the nonlinearity of the optimization process.

Results obtained from this and several additional comparisons with SEPSPOT allowed for sufficient confidence in the direct method to justify its use as the primary tool for trajectory analysis in this study. Additional comparisons are omitted for brevity.

C. Fixed Variables and Key Assumptions

The ground rules and assumptions used in this study include a series of control variables that are held constant throughout all SE-EOR trials. This is done both for simplicity and to ascertain the sensitivity of overall performance to changes in major mission parameters (C_3, I_{sp}, and cryogenic boil-off). Some of these control variables were later relaxed, where noted, to assess their implications. The primary assumptions of this study are presented in Table 2.

In addition to the assumptions noted in Table 2, all trials were arbitrarily assumed to begin on 1 January 2015, for consistency. Both radiation-induced solar cell degradation and Earth shadowing were modeled in each trial. Continuous thrusting is also assumed, with no coast arcs except when spacecraft are in eclipse. Earth oblateness and third-body perturbations were ignored in the interests of robust program convergence with both SEPSPOT and the direct method.

Atmospheric drag effects were also ignored, though it is noted that such effects may be of significant concern for larger SE tugs with low ballistic coefficients. However, for the purposes of this study, the

Table 2 Primary assumptions used in SE-EOR analyses

Quantity	Assumption
Solar array type	Gallium arsenide (GaAs)
Solar array specific mass	9 kg/kW
Solar cell shield thickness	16 mm
Thruster type	Hall
Thruster specific mass	2 kg/kW[a]
Power-processing system specific mass	4 kg/kW[a]
Trapped (unusable) fuel	5%
Hydrogen/oxygen engine I_{sp}	465 s
Methane/oxygen engine I_{sp}	370 s
Solar electric payload adapter mass	5% of payload mass
Solar electric fuel-tank fraction	10% of payload mass
Chemical rocket-stage fraction	20% of propellant mass

[a]Values from [2].

most optimistic assumptions as to SE performance were made, such that the implications of coupling chemical-stage boil-off could be assessed under best-case circumstances; hence, drag effects are not considered. It is further noted that in most LEO–HEEO orbit raises, the perigee altitude is raised quickly and is only returned to lower altitudes once the spacecraft neared its final target apogee. This is as a result of the optimization methods used in both SEPSPOT and the direct method.

For all LEO–HEEO trials, only semimajor axis, eccentricity, and inclination were specified to define the initial and final orbits. The beginning and end values of ascending node longitude, argument of perigee, and true anomaly were unconstrained. Furthermore, all spacecraft were allowed six degrees of freedom with no attitude constraints imposed on thrust direction, in the interest of maintaining mission generality.

Finally, and perhaps most specifically, the power-to-mass ratio of all spacecraft modeled in this study was used as a control variable and chosen to be 5 W/kg, consistent with the upper end of optimistic assumptions for SE spacecraft [2,4]. There is a well-known tradeoff between specific power and increasing spacecraft power subsystem mass [1]. For reasons discussed later, values below 5 W/kg reduce SE performance significantly when cryogenic upper stages are assumed for interplanetary injection.

D. Data Collection and Reduction Methods

The basic methodology of this study was as follows: increasing LEO–HEEO orbit raises were methodically targeted, at varying values of SE I_{sp}, with data from each trial collected and tabulated in a spreadsheet program via a postprocessing algorithm written in Fortran. Although trajectory simulation and optimization was perhaps the most challenging aspect of this study, the majority of significant results were obtained from postsimulation data reduction and were thus easy to manipulate to study the sensitivity of SE-EOR to changing system characteristics.

Table 3 presents the minimum required inputs and outputs of both SEPSPOT and the direct method used in this study. In addition to the input quantities listed in Table 3, either the initial costate vector guess (SEPSPOT) or costate weighting functions (SEPDOC) were also required as user inputs. In trials using the direct method, the latter only needed to be set once for all LEO–HEEO simulations, after which only the target orbit, TOF, and spacecraft characteristics were varied.

During each run, both programs assume that the entire initial spacecraft mass can be consumed as fuel if necessary. Once the final mass and power were obtained, the available, or non-SE mass, was calculated as

$$m_3 = \frac{m_2 - (f_{\text{fuel}} + f_{\text{tank}})(m_1 - m_2) - P(\rho_{\text{PPU}} + \rho_{\text{Th}} + \rho_{\text{AR}})}{(1 + f_{\text{adpt}})} \tag{17}$$

where m_1, m_2, and m_3 are the pre-, post-, and non-SE spacecraft masses in kilograms; P is the total spacecraft power in kilowatts; ρ_{PPU}, ρ_{Th}, and ρ_{AR} are the specific power-processing, thruster, and array masses in kilograms per kilowatt; and f_{fuel}, f_{tank}, and f_{adpt} are the unused fuel, tank, and payload adapter mass fractions, respectively.

Table 3 Minimum required input variables and output variables for SEPSPOT and the direct method

Input variables	Output variables
Initial classical orbital elements	Final semimajor axis, km
Estimated time of flight, days	Final eccentricity
Target orbital elements	Final inclination, deg
Maximum time of flight, days	Final spacecraft mass ratio
Spacecraft initial mass, kg	Final spacecraft power fraction
Spacecraft initial power, kW	Time of flight, days
Solar electric I_{sp}, s	
Thrust efficiency	
Solar array type (GaAs or Si)	

The velocity change required for interplanetary injection from the final HEEO after the SE stage is detached can be determined from the trajectory C_3 and the final perigee altitude of the transfer, from which the required non-SE mass ratio can be calculated from the ideal rocket equation:

$$R = \exp\left(\frac{\Delta v}{g I_{\text{sp}}}\right) \tag{18}$$

During the SE orbit-raising phase of the mission, the rate of cryogenic propellant boil-off in the chemical upper stage can be written as the integral

$$\kappa = \int_0^{TOF} \kappa(t)\, \mathrm{d}t \tag{19}$$

where the integration limits are taken as the time of stage delivery, $t = 0$, and the total orbit-raise time TOF. For the purposes of this study, we define a time-averaged rate of boil-off $\bar{\kappa}$, which is varied as a monthly percentage of propellant loss for hydrogen/oxygen bipropellant; in this study, generally $0 \le \bar{\kappa} < 0.03$ (though it is noteworthy that this assumed range is extremely optimistic). Using this time-averaged boil-off rate, we define a propellant loss ratio λ to characterize the required chemical injection system:

$$\lambda = \frac{P_0}{m_3} = \frac{R - 1}{R - (\bar{\kappa} + f_{\text{stage}})} \tag{20}$$

where P_0 is the total bipropellant mass delivered to orbit at $t = 0$. The final payload mass m_4 can then be written in terms of the propellant loss ratio as

$$m_4 = m_3[1 - (1 + f_{\text{stage}})\lambda] \tag{21}$$

and the payload ratio PR for the mission is simply

$$PR = \frac{m_4}{m_1} \tag{22}$$

which is the quantity that is generally desirable to maximize.

IV. Discussion of Results

A. Upper-Stage Boil-Off Impact

Based on the methodology outlined previously, a number of LEO–HEEO transfers were analyzed at varying SE I_{sp} values. All spacecraft were assumed to start in a 51.6-deg-inclination, 400-km circular orbit, consistent with the NASA Johnson Space Center study [4]. This initial orbit is also approximately the same as the orbit of the International Space Station and is chosen to reduce radiation fluence. From this initial orbit, spacecraft slowly spiral out to coplanar final HEEOs with apogee altitudes ranging from 5000 to 140,000 km, with final perigee altitudes of 800 km in all cases, as in [4]. A maximum target apogee of 140,000 km was chosen on the basis of program convergence, which became extremely difficult using either SEPSPOT or the direct method for eccentricities exceeding 0.9.

SE-EOR is highly effective when cryogenic boil-off of upper-stage propellant is not considered. Figure 4 illustrates this, in which PR is plotted against SE I_{sp} on lines of constant target apogee altitude for launching a payload onto a near-minimum-energy trans-Mars injection ($C_3 = 16\ \text{km}^2/\text{s}^2$). As Fig. 4 shows, the effectiveness of SE-EOR consistently increases for increasing SE I_{sp} values when upper-stage boil-off is not considered. The maximum achievable PR from an all-chemical hydrogen/oxygen is also included in Fig. 4 for reference. In the all-chemical scenario, a large chemical propulsion stage is assumed to deliver an interplanetary payload to near-Earth escape ($C_3 \approx 0\ \text{km}^2/\text{s}^2$), from which a smaller integral stage performs the final interplanetary injection maneuver. The idea of staging an interplanetary injection maneuver at the sub-Earth escape point was first developed by Meissinger et al. [11] and can greatly

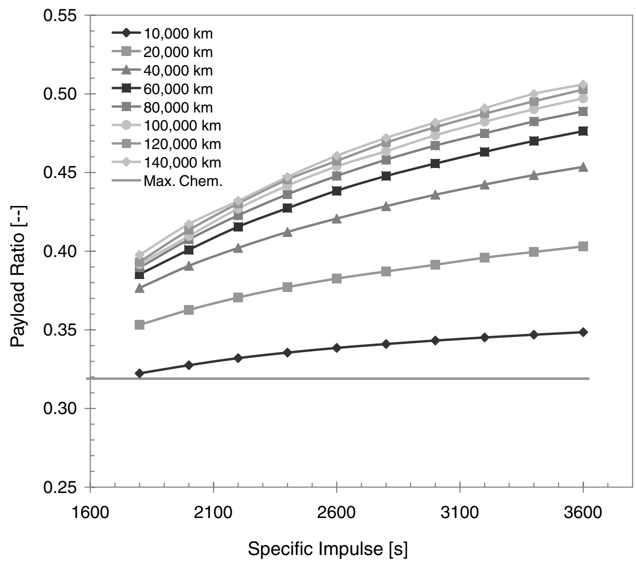

Fig. 4 **Payload ratio vs SE I_{sp} for Mars missions as a function of target apogee altitude ($C_3 = 16\ \mathrm{km}^2/\mathrm{s}^2$, no boil-off).**

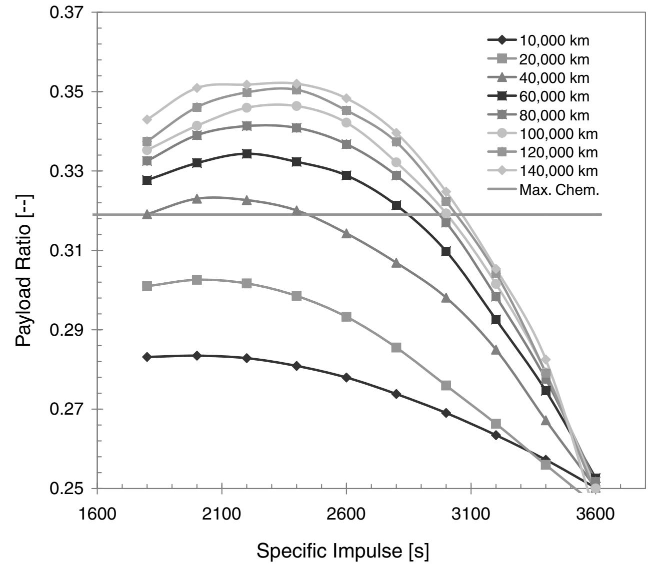

Fig. 6 **Payload ratio vs SE I_{sp} for Mars missions as a function of target apogee altitude ($C_3 = 16\ \mathrm{km}^2/\mathrm{s}^2$, boil-off rate is 3% per month).**

increase the relative payload gain achievable with all-chemical injection systems. This launch mode is particularly effective for high C_3 missions, because the need to accelerate an otherwise parasitic large upper stage through the entire injection maneuver is avoided. As noted previously, all SE-EOR scenarios analyzed consider both radiation power degradation and Earth-shadowing effects, but with Earth oblateness effects ignored.

However, when upper-stage propellant boil-off effects are considered, the PR benefit of increasing SE-EOR I_{sp} begins to diminish rapidly. Figures 5 and 6 illustrate this, in which increasing monthly boil-off rates are 1 and 3%, respectively. The same chemical injection line from Fig. 5 is included for reference and remains unaffected by boil-off effects, due to the assumption of impulsive all-chemical interplanetary injection. I_{sp} optimums begin to emerge for cryogenic boil-off rates as low as 1% per month for trans-Mars injections using SE-EOR; as rates climb higher, SE-EOR ceases to be competitive with all-chemical injection systems, even at highest I_{sp} values and target altitudes. At a boil-off rate of 4%, no performance advantages exist at all to the SE-EOR mission mode for Mars. This situation becomes even further exacerbated when higher C_3 missions are considered. Figures 7 and 8 show similar curves for trans-Jupiter injections at cryogenic boil-off rates of 1 and 2% per month, respectively.

These results indicate that the benefits of SE-EOR are quickly marginalized or eliminated by even small cryogenic boil-off rates and that SE I_{sp} maximums begin to emerge with increasing boil-off rates. This results from the inverse relationship between SE exhaust velocity and thrust [Eq. (15)] and the ensuing result that higher-I_{sp} electric engines require longer flight times to any given target HEEO. Because higher I_{sp} SE tugs will have correspondingly lower thrust levels, orbit-raising times will be longer, resulting in greater cryogenic propellant boil-off. Increasing C_3 also results in diminished performance and SE-EOR optimums when boil-off is accounted for, because the performance burden placed on the cryogenic upper stage is exponentially greater. Thus, although SE-EOR appears highly advantageous when considered independently of the chemical upper stage used for final injection, the overall mission is nevertheless extremely sensitive to increasing propellant boil-off rates and interplanetary launch energy when the performance of both stages are coupled.

Although Figs. 4–8 demonstrate the sensitivity of SE-EOR performance to variations in cryogenic boil-off and C_3, it is

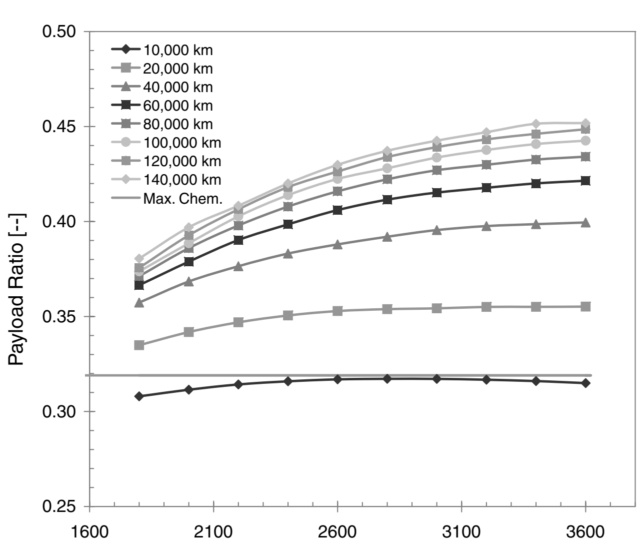

Fig. 5 **Payload ratio vs SE I_{sp} for Mars missions as a function of target apogee altitude ($C_3 = 16\ \mathrm{km}^2/\mathrm{s}^2$, boil-off rate is 1% per month).**

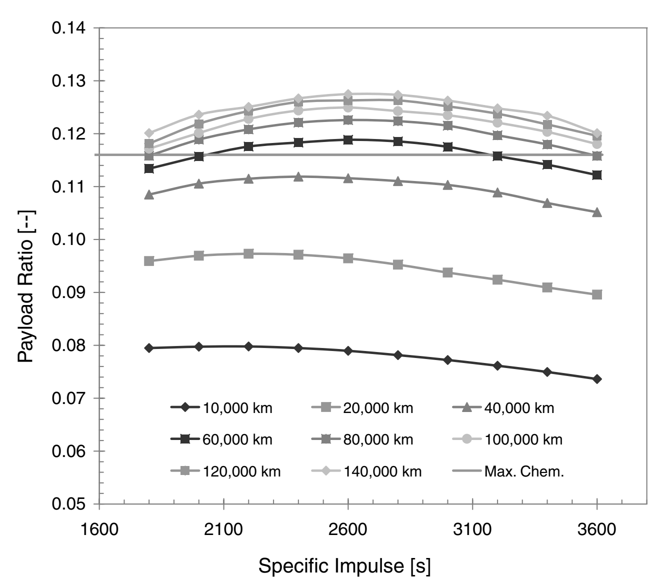

Fig. 7 **Payload ratio vs SE I_{sp} for Jupiter missions as a function of target apogee altitude ($C_3 = 87\ \mathrm{km}^2/\mathrm{s}^2$, boil-off rate is 1% per month).**

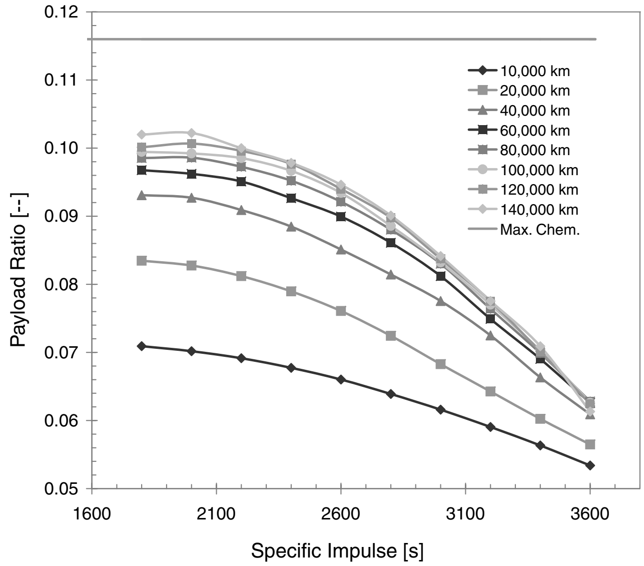

Fig. 8 Payload ratio vs SE I_{sp} for Jupiter missions as a function of target apogee altitude ($C_3 = 87\ \mathrm{km^2/s^2}$, boil-off rate is 2% per month).

noteworthy that such systems are also extremely sensitive to percent variations in many other system assumptions, such as stage fractions for chemical upper stages. Although percent variations in such parameters cause shifts in the graphs, the relative relationship between SE-EOR and all-chemical injections remain unaltered when such changes are applied to both. For this reason, analysis of such effects is omitted for brevity.

B. Space-Storable Stages

Perhaps the most intuitive option for mitigating the issues associated with cryogenic propellant boil-off is to use space-storable chemical propellants for interplanetary injection. For the purposes of this analysis, space-storable propellants are defined as combinations that are assumed to be largely insensitive to boil-off issues, including both noncryogenic hypergolic bipropellants and less-cryogenic combinations such as methane/oxygen.

Figure 9 shows SE-EOR I_{sp} curves compared with an all-chemical injection system when hypergolic monomethyl-hydrazine/nitrogen-tetraoxide (MMH/NTO) propellants are used for interplanetary injection to Mars. MMH/NTO propellants are assumed to have a steady-state specific impulse of 325 s [12]. Although the SE I_{sp} optimums arising from boil-off issues were eliminated, the maximum achievable payload ratio was nevertheless marginalized by using a lesser-performance propellant combination for the final interplanetary injection maneuver. Figure 10 shows that improvements can be obtained by using methane/oxygen with $I_{sp} = 370$ s. In Fig. 10, the use of methane/oxygen for trans-Mars injection is approximately competitive with a boil-off-degraded hydrogen/oxygen injection system. However, although a high-performance space-storable combination such as methane/oxygen is advantageous for relatively low C_3 missions, their benefit quickly disappears for higher C_3 requirements such as expedited flights to Mars or low-energy transfers to Jupiter. Figure 11 illustrates this effect for the latter case. Because the C_3 for a given mission dictates the energy requirements of the chemical upper stage in SE-EOR, lower-performance systems are particularly susceptible to increasing interplanetary launch energies. In Fig. 11, even the use of high-performance methane/oxygen propellants does not produce an SE-EOR mission mode that is competitive with an all-chemical injection system.

C. Relative Payload Gain Rate

Payload ratio is a reasonable quantity to maximize in space mission design when time is not considered an issue. However, in reality, time has an inherent cost that must be considered, particularly

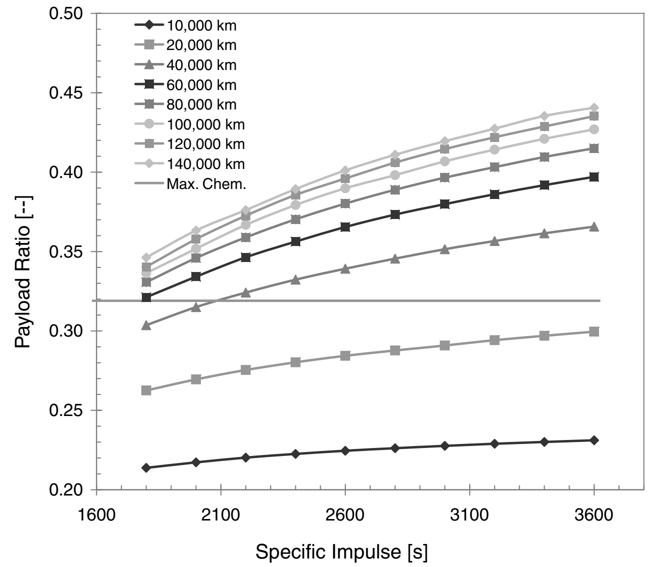

Fig. 9 Payload ratio vs SE I_{sp} for Mars missions as a function of target apogee altitude ($C_3 = 16\ \mathrm{km^2/s^2}$, no boil-off, MMH/NTO bipropellant).

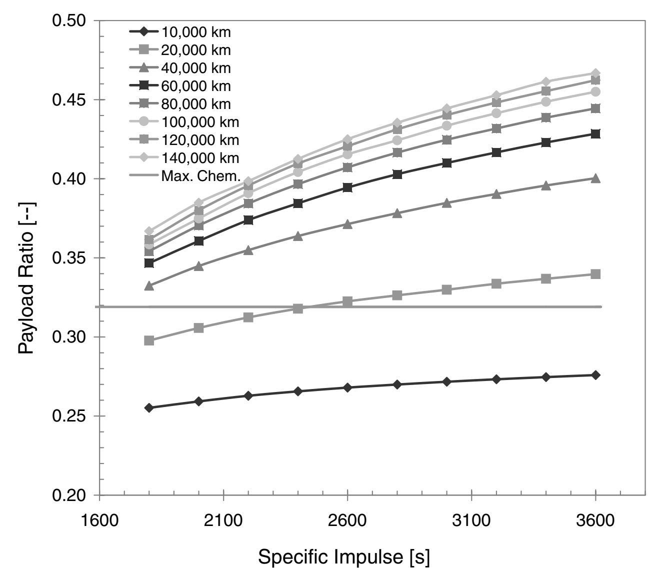

Fig. 10 Payload ratio vs SE I_{sp} for Mars missions as a function of target apogee altitude ($C_3 = 16\ \mathrm{km^2/s^2}$, no boil-off, CH_4/O_2 bipropellant).

in commercial missions. Thus, it is often the case that the aim of the mission planner is to reduce costs associated with lengthy mission times by maximizing transportation rate (kilograms gained/time) rather than overall payload ratio [1].

To analyze time considerations in SE-EOR, we previously introduced the concept of relative payload gain rate δ to quantify the payload ratio gained per unit of mission operation time when compared with competing all-chemical injection options, which are assumed to perform interplanetary injection instantaneously. By this metric, the best possible interplanetary launch mode is not necessarily the one that maximizes payload ratio, but rather that which results in the greatest amount of payload gain with respect to instantaneous injection per day of mission operation.

Figure 12 shows the relative payload gain rate for SE-EOR missions to Mars as a function of SE I_{sp}, again on contours of constant apogee altitude. Even without boil-off effects considered, the relative payload gain rate metric in SE-EOR missions gives rise to optimal I_{sp} values. Figure 13 shows that these optimums become even more pronounced when boil-off effects are accounted for. For

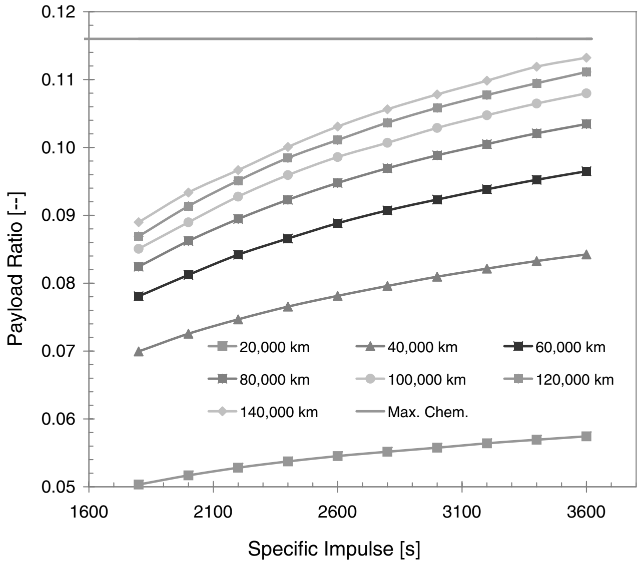

Fig. 11 Payload ratio vs SE I_{sp} for Jupiter missions as a function of target apogee altitude ($C_3 = 87\ \mathrm{km}^2/\mathrm{s}^2$, no boil-off, CH_4/O_2 bipropellant).

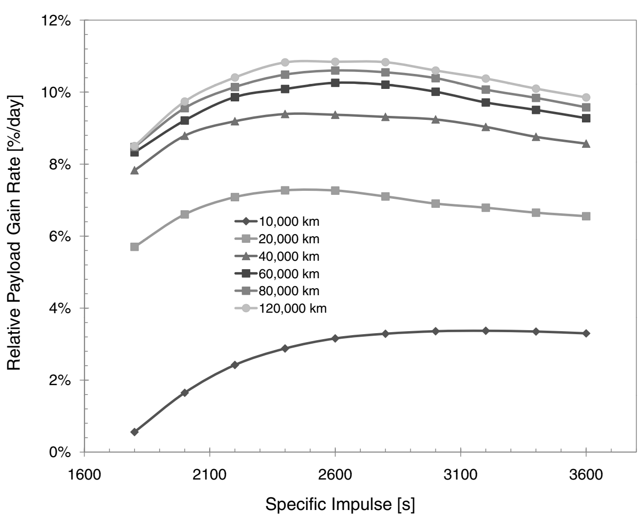

Fig. 12 Relative payload gain rate for Mars missions ($C_3 = 16\ \mathrm{km}^2/\mathrm{s}^2$, no boil-off).

missions requiring higher C_3, similar optimums can be found to emerge when evaluating mission designs by the δ metric, often producing negative relative payload gain rate values for high C_3 opportunities, as shown in Fig. 13.

The I_{sp} optimums associated with relative payload gain rate can be understood by considering the relationships between payload ratio, the final target HEEO, and its associated flight time. For increasing target altitudes, and thus for increasing flight times, the *PR* increases attainable with SE-EOR begin to plateau. This effect can be seen by moving vertically through the series of constant apogee contours in Figs. 5–11. Beyond a certain target altitude, the benefits of increasing HEEO apogee increasingly diminish. Thus, on a per-unit-time basis, a point comes when substantial PR increases simply require too much time to yield high relative gains per day. This effect is further exacerbated by increasing boil-off rates and C_3, in which payload benefits not only plateau with increased operation time, but actually begin to diminish.

Thus, although certain SE-EOR systems may maximize attainable payload ratio, the relative PR gains per unit of mission time often lead to different design point optimums. Mission planners must therefore consider the extent to which transportation rates and relative gains are significant in a particular SE-EOR design.

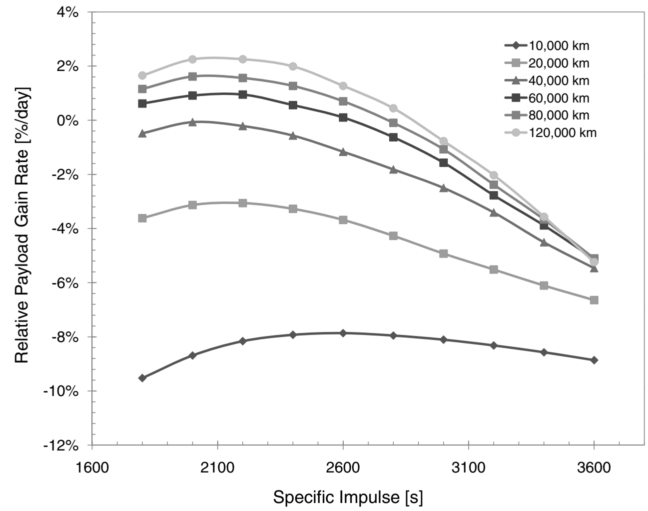

Fig. 13 Relative payload gain rate for Mars missions ($C_3 = 16\ \mathrm{km}^2/\mathrm{s}^2$, boil-off rate is 3% per month).

D. Human-Class Missions and SE Tug Reuse

In this section, we evaluate the larger class of SE-EOR missions as outlined in NASA's Mars DRM 3.0 [2–4], in which human-class (~50-ton) payloads are transferred from LEO to HEEO and injected trans-Mars by a small hydrogen/oxygen cryogenic upper stage. The SE tug designed by NASA would employ Hall thrusters with a variable specific impulse between 2000 and 3000 s.

The NASA tug was analyzed by assuming that the thrust efficiency varied with I_{sp} during flight, according to Eq. (16). The variable nature of I_{sp} was factored into the optimization of the NASA tug's trajectory, and a time-varying specific impulse profile evolved during orbit raising that lowered I_{sp} to increase thrust for passage through the Van Allen radiation belts.

Figure 14 compares the achievable payload ratios of the NASA SE tug with an all-chemical injection system as a function of staging altitude, for which it is assumed that either SE or initial chemical staging occurs, respectively, in each scenario. Performance curves with boil-off rates of 0 and 1% per month are shown in Fig. 14. With boil-off accounted for, the performance of the SE injection system is greatly marginalized. The use of a space-storable methane/oxygen upper stage with zero boil-off gives little performance gain above a boil-off-susceptible cryogenic injection system.

In addition to the boil-off considerations noted earlier, further complications arise in larger SE-EOR missions as a result of the sheer magnitude of the required tug mass. The development of SE tugs capable of transporting human-class payloads will require significant capital investment and infrastructure placed in LEO. Consequently, reuse of the SE tug for several successive orbit raises is specified in the NASA study as highly desirable, both for cost amortization

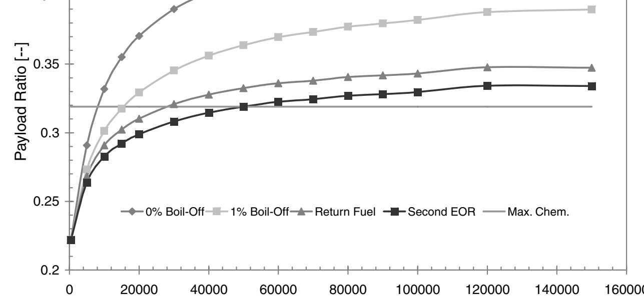

Fig. 14 NASA SE tug performance curves for Mars missions ($C_3 = 16\ \mathrm{km}^2/\mathrm{s}^2$).

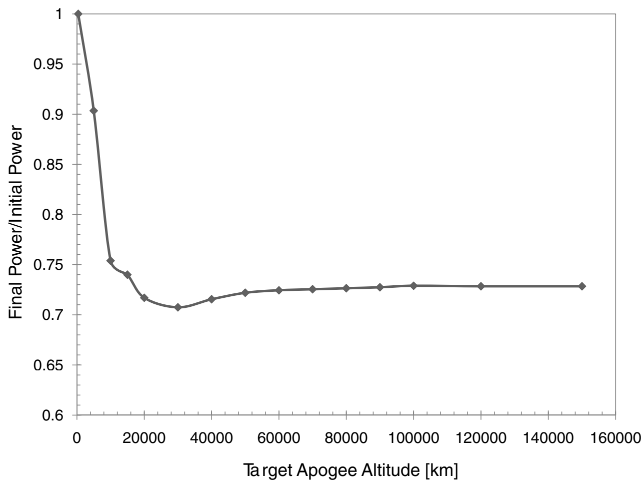

Fig. 15 SE power degradation as a function of target altitude.

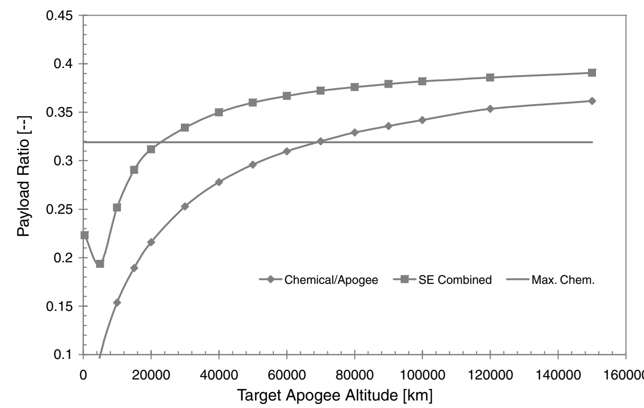

Fig. 16 Comparison of SE and chemical plane changes for Mars missions ($C_3 = 16\ \mathrm{km^2/s^2}$).

purposes and to avoid the otherwise problematic marginal cost of having to redevelop a new SE tug for each mission. This is a prospect that is far more realistic for small missions than for larger missions.

To reuse the SE tug for subsequent orbit raises, a sufficient amount of SE propellant must be held in reserve to return the tug to LEO for subsequent orbit raises. However, the reserve fuel requirement acts to further marginalize the benefits of SE-EOR. This is shown in the corresponding curve in Fig. 14, in which the benefit of using SE-EOR as opposed to all-chemical injection has almost completely been eliminated. In the analyzed mission scenario, the time of flight required for return is generally on the order of 25% of the orbit-raising time, because the tug does not have to return any payload to LEO.

Although the proposed NASA mission does nevertheless still offer some advantage over chemical propulsion, it is important to consider the implications of recycling the tug. Consider Fig. 15, which shows the SE tug's solar array power output as a function of target apogee altitude. By the end of the initial orbit-raising phase at maximum altitude, the available power has been degraded by approximately 27.5%. Returning to Fig. 14, we can see that although the return trip to LEO is expeditious and therefore does not further degrade the solar arrays significantly, the reduced power level nevertheless has a serious impact on the performance of a second orbit raise as a result of increased time of flight. It should be noted that in Fig. 14, the recycled SE mass is discounted from the initial mass in LEO figure to the benefit of payload ratio. However, even this consideration notwithstanding, the second orbit raise does not offer any apparent advantages over all-chemical injection.

Finally, in addition to the technical difficulties associated with construction, deployment, use, and reuse of massive SE tugs, there is a necessary reality check that must be performed with respect to procuring the necessary amounts of xenon fuel required for each orbit raise. The NASA study requires approximately 40 t of xenon per orbit raise (and thus, per year, assuming full capital use). However, the current total annual production of xenon globally via fractional distillation is only on the order of 35 t per year [13], of which a significant fraction in turn is used for medical purposes. Although this annual production quantity may only reflect the global market for xenon and not speak to the surge capabilities of industry to produce greater quantities, the fact that a human-class SE tug as described by NASA would require global xenon production to approximately double may also weigh against the viability of this concept.

E. Optimum Plane Change

The majority of SE-EOR missions considered in this study were chosen to begin in a 51.6-deg-inclination LEO. This inclination is chosen as a balance between global launch access capabilities and the desire for high-inclination spiraling to minimize radiation-induced solar panel degradation. However, a 51.6-deg inclination is not optimal for launching interplanetary missions, and a plane change maneuver into the ecliptic is required before interplanetary launch in such scenarios. This is a frequently cited criticism of the International Space Station, which lies in the 51.6-deg orbital plane and is thus problematic in supporting interplanetary missions.

In this section, we consider two different plane change methods for SE-EOR missions: a combined maneuver using the SE propulsion system during orbit raising and an all-chemical maneuver performed by the payload upper stage at apogee after SE jettison and before interplanetary injection. The SE combined maneuver is unconstrained in all respects (except for the target final inclination), and the chemical plane change assumes that the lines of apsides are aligned between the two final HEEOs in question. Figure 16 shows the achievable payload ratios for each approach, again with an all-chemical injection maneuver plotted for reference for trans-Mars injections. The case shown employs an SE tug with $I_{\mathrm{sp}} = 2200$ s, though variable I_{sp} values present comparable curves, with only the relationship to all-chemical performance affected, as in Sec. IV.A.

Regardless of whether boil-off effects are considered, in all cases, the combined SE plane change yields both higher payload ratios and relative payload gains when compared with the chemical plane change applied at apogee. Although the SE plane change curve in Fig. 16 shows a slight decrease in PR for low altitudes, this only occurs because the majority of the plane change maneuver takes place deep within the Earth's gravity well. As a consequence, the low-thrust propulsion system is significantly affected when the plane change maneuver is constrained to occur over a relatively short interval at low altitude. In trajectory simulation and analysis, both SEPSPOT and the direct method optimize the combined plane change maneuver to minimize power degradation. As a result, a significant portion of the inclination change is performed only after passage through regions of high radiation flux. End-of-life power and flight time differences between the SE combined and chemical/apogee plane change scenarios are negligible.

The optimal inclination change between noncoplanar orbits is not necessarily applied exclusively at apogee for conventional transfers [14]. Similarly, it is noted here that the truly optimal plane change maneuver with a combined SE/chemical propulsion system may not be found in the exclusive use of either system alone. Additionally, because HEEOs with extremely high eccentricities (greater than 0.9) could not be analyzed effectively with the optimization methods employed in this study, the issue of plane changes between LEOs and extremely high HEEOs was not investigated. It is expected that HEEOs with significantly higher apogees than those studied would result in much more complex scenarios, in which the impact of lunar and solar perturbations would become increasingly important.

V. Interplanetary Low-Thrust Rocket Equation

The methodology used to derive previous results involved the assumption of fixed power-to-mass ratios for reference spacecraft and involved detailed trajectory simulation of each orbit raise to increasingly high-altitude HEEOs to derive system performances, SE velocity change requirements, and flight times. Each trajectory was time-optimized at fixed power-to-mass spacecraft ratios.

However, when the power system size of an SE-EOR mission itself becomes an optimization variable or when a certain flight time to a desired HEEO is specified, a new analysis methodology is required. In this section, we modify the low-thrust rocket equation to allow for power-free SE-EOR sizing, while also coupling the impacts of cryogenic propellant boil-off and interplanetary launch energy.

Consider a solar electric tug in which the inert mass is a function of the required thrust and the tankage mass is some fraction of the required SE propellant. Assuming a constant propellant mass flow rate, the SE tug system mass will be

$$m_{\mathrm{SE}} = \frac{c^2 m_{\mathrm{prop}}(1 + f_{\mathrm{tank}} + f_{\mathrm{trapped}})}{2\alpha\eta t} \tag{23}$$

where $\alpha = 1/(\rho_{\mathrm{PPU}} + \rho_{\mathrm{Th}} + \rho_{\mathrm{AR}})$. The part of the overall SE-EOR system mass that is not associated with the SE tug (i.e., the payload and interplanetary injection system) can be written as

$$m_{\text{non-SE}} = m_0 - m_{\mathrm{SE}} = \frac{m_{\mathrm{payload}}(1 + f_{\mathrm{adpt}})}{1 - (1 + f_{\mathrm{stage}})\lambda} \tag{24}$$

where λ is the propellant mass fraction defined in Sec. III and, because it contains the required injection mass ratio for interplanetary injection, characterizes the entire post-EOR mission phase. By combining the preceding equation with the ideal rocket equation for the orbit-raising phase of the overall mission and by rearranging the preceding expression, we arrive at the interplanetary low-thrust rocket equation:

$$\frac{m_{\mathrm{payload}}}{m_o} = \left[\left(\frac{1 - (1 + f_{\mathrm{stage}})\lambda}{1 + f_{\mathrm{adpt}}}\right)\right]\left[\exp\left(-\frac{\Delta v}{c}\right) - 1 + \exp\left(-\frac{\Delta v}{c}\right)\left(\frac{c^2(1 + f_{\mathrm{stage}} + f_{\mathrm{trapped}})}{2\alpha\eta t}\right)\right] \tag{25}$$

Assuming that the stage, adapter, and trapped fuel fractions are negligibly small, we can write Eq. (25) in a more compact form as

$$\frac{m_{\mathrm{payload}}}{m_o} = (1 - \lambda)\left[\exp\left(-\frac{\Delta v}{c}\right) - 1 + \exp\left(-\frac{\Delta v}{c}\right)\left(\frac{c^2}{2\alpha\eta t}\right)\right] \tag{26}$$

This and other versions of the low-thrust rocket equation require that one has a reasonable guess as to the velocity change required between two given Earth orbits, which can be easily approximated for circle-to-circle transfers [14]. However, the velocity change for a LEO–HEEO transfer cannot be so easily estimated and is itself a function of the assumed duty cycle for the transfer and system in question.

VI. Earth-Eclipse-Evading Transfers

We demonstrated in Sec. IV that the potential of SE-EOR for interplanetary missions can be severely degraded by propellant boil-off in the cryogenic upper stage used for injection, which in turn is a direct function of orbit-raising flight time.

During eclipse periods, the method of analysis used in this study assumes that no power is received by electric thrusters and that any secondary power available is used exclusively for maintaining other subsystems. Thus, no thrusting is assumed to occur during eclipse phases. In due course, SE-EOR missions that experience eclipses have correspondingly longer flight times, on the order of 100 days or greater, depending on the specific inclination of the transfer and characteristics of the SE tug.

However, if SE-EOR transfers could be found that minimize or eliminate the eclipse phases of a given mission, then transfer times could potentially be expedited by months, which would result in corresponding reductions in propellant boil-off and thus higher payload ratios and payload rates from LEO to HEEO.

As a means of reducing or eliminating Earth-eclipse times in SE-EOR missions, we introduce the concept of an Earth-eclipse-evading (E^3) transfer, which, by this definition, is a non-sun-synchronous transfer in an elliptical plane that only just avoids intersecting the Earth's umbra/penumbra at perigee. The concept of E^3 orbits was first investigated by Wehrle and Beaudette [15], in which both sun-synchronous and non-sun-synchronous families of fixed eclipse-evading orbits were considered. Although for any non-sun-synchronous orbit, the orbital plane must necessarily fall into alignment with the sun–Earth shadow line at some point and thus must eventually cross into the Earth's shadow, this does not necessarily mean that the spacecraft orbiting in this plane will pass into eclipse itself.

To illustrate this principle with a simple example, consider an SE tug spiraling a payload outward from an initial circular polar orbit, as shown in Fig. 17. In this figure, we specify an SE transfer such that there comes a point at which, at either the vernal or autumnal equinox, the tug is spiraling out from a perigee on the sun side of the Earth-sun line. In such a scenario, at the time at which the Earth's shadow passes through the orbital plane, the transfer has a sufficiently large semimajor axis such that the Earth's shadow passes through the spiral plane because of the motion of the Earth around the sun during the half-orbits before and after equinox. If the SE tug is appropriately positioned at this time, the spacecraft can essentially perform a "corkscrew" maneuver around the Earth's shadow and continue evading subsequent eclipse.

Many additional considerations are required for designing stable, long-lived, circular E^3 orbits, particularly in the context of orbital perturbations. Fortunately, however, for SE transfers that are transient in nature, the effects of perturbations to the E^3 transfer can be largely ignored or mitigated by the SE propulsion system. Indeed, it may even be desirable to use the SE propulsion system to artificially progress the transfer longitude of the ascending node to further aid in avoiding eclipses at high inclinations.

Figure 18 shows the payload ratio gains and flight time reductions achievable via an Earth-eclipse-evading transfer with an SE $I_{\mathrm{sp}} =$ 1800 s launching a Mars-bound payload. Although flight time reduction can be used as a means of increasing payload and transportation rate via E^3 transfers, it is also noted that higher specific impulse values can also be adopted to further benefit payload ratios at flight times equal to frequently eclipsed transfers.

The principle of Earth-eclipse evasion in SE-EOR may hold significant promise when higher-inclination orbits are accessible for establishing an initial spiral plane. However, the requirement for a high-initial-inclination starting orbit is recognized as a possible drawback of such a transfer, depending on the latitude available for spacecraft launch. This paper represents the first investigation of

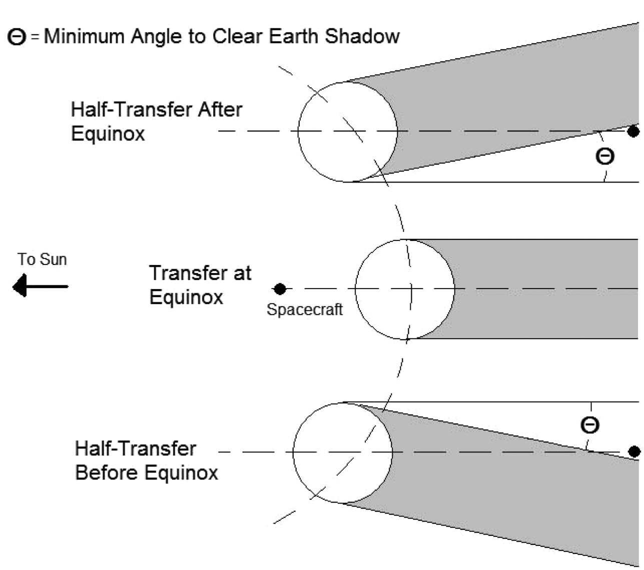

Fig. 17 Earth-eclipse-evasion transfer geometry at equinox.

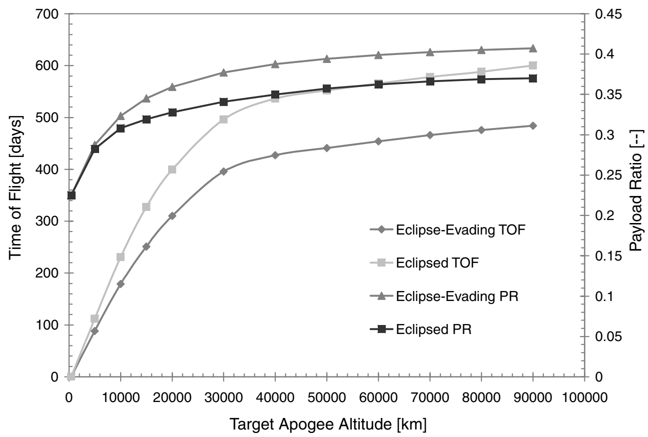

Fig. 18 Comparison of E^3 and eclipsed SE transfers for Mars mission ($C_3 = 16\ \mathrm{km^2/s^2}$).

using E^3 behavior to the benefit of an SE transfer. However, the potential of this approach requires further investigation in the context of more specific mission designs.

VII. Conclusions

An end-to-end evaluation of the potential of SE-EOR for accomplishing interplanetary missions is discussed. Although representing a potentially promising way of conducting interplanetary injections, it is nevertheless shown that several factors can act to mitigate the relative gains achievable by using SE-EOR with respect to competing options.

A direct method of solar electric trajectory time optimization is discussed and validated for transfers to high-energy orbits. Subsequently, an algorithm is presented that couples the effects of upper-stage cryogenic propellant boil-off considerations to overall SE-EOR mission analysis. It is found that propellant boil-off in chemical upper stages during SE orbit raising can severely marginalize the potential of solar electric stages for increasing interplanetary payload ratios, particularly for high-energy launch opportunities. It is also shown that I_{sp} optimums begin to emerge for SE stages as even optimistically small cryogenic boil-off rates are introduced. This effect is otherwise not apparent without coupling the performance of solar electric and chemical stages. Although space-storable injection stages are presented as a possible alternative to mitigate detrimental boil-off effects, it is shown that their comparatively lower performance (particularly for high C_3 missions) limits their potential. This suggests that mitigating propellant boil-off for high-performance cryogenic stages is a favorable approach to using lower-performance propellants.

Because time has an inherent cost in space missions, the impact of time is evaluated via the relative payload gain rate metric, which evaluates the relative gains attainable with SE-EOR over chemical injection systems per unit of mission time. This metric leads to rate-optimal I_{sp} values regardless of whether propellant boil-off is factored into the analysis.

Because the preponderance of available literature on SE-EOR exists for larger human-class missions, the potential of using large SE tugs to dispatch more significant payloads to interplanetary transfers is evaluated in the context of the preceding issues. In addition, several more considerations intrinsic to larger spacecraft, such as the desirability of reuse, are also considered. It is shown that the reserve fuel required for tug return to LEO can severely limit the relative payload gain of SE-EOR over competing all-chemical options at much lower payload rates and much higher capital investments. It is further argued that power degradation makes SE tug reuse nonviable and that the economic considerations of propellant procurement may result in larger SE-EOR missions being untenable with existing technology. However, SE-EOR nevertheless appears to hold considerable promise for scenarios in which capital investments in mission hardware are sufficiently small as to make abandoning the solar electric stage acceptable after one orbit raise.

The issue of plane changes from low-radiation spiral to interplanetary injection planes is addressed. It is shown that a plane change maneuver combined with the SE-EOR phase of each mission yields higher payload ratios and relative payload gains than plane changes executed by payload upper stages following SE separation at apogee.

It can be foreseen that for some SE-EOR missions, power system mass may become an optimization variable and specific velocity change and flight times may be desired. For such cases, an augmented variant of the low-thrust rocket equation is presented that couples propellant boil-off and C_3 for a given mission in a single variable, referred to as the propellant loss ratio.

A novel form of transfer, referred to as an Earth-eclipse-evading (E^3) transfer, is introduced and investigated. The E^3 transfer holds the potential of reducing SE-EOR transfer times by hundreds of days when higher-inclination orbits are accessible. The E^3 transfer is only evaluated in a preliminary sense, and it is recommended that further study be undertaken to fully ascertain its potential for increasing payload ratios and relative payload gains in SE-EOR missions.

Finally, because of the high demonstrated sensitivity of the nonlinear SE-EOR problem to minute variations in systems-level assumptions, it is recommended that further study be performed into SE-EOR mission designs, including the use of more detailed propellant boil-off models and the inclusion of additional systems-level parameters such as SE specific impulse as optimization variables in trajectory analysis. Should SE-EOR missions such as those described herein be employed in future interplanetary missions, a new set of dedicated tools beyond those currently available will be required for analysis, such that this potentially highly beneficial method of conducting interplanetary missions can be fully characterized and understood.

Acknowledgments

The authors would like to acknowledge the following individuals for their contributions to this study: John Riehl, the Solar Electric Propulsion Steering Program for Optimal Trajectory (SEPSPOT) point of contact at NASA Goddard Research Center; Craig Kleuver of the University of Missouri—Columbia, original developer of the direct optimization methodology employed in this study; Victor Wehrle of the Canadian Space Agency (retired); Bruce Burlton of Carleton University; and Kyle McMartin, who assisted in compiling SEPSPOT for our use.

References

[1] Oh, D. Y., Randolph, T., Kimbrel, S., and Martinez-Sanchez, M., "End-to-End Optimization of Chemical-Electric Orbit Raising Missions," *Journal of Spacecraft and Rockets*, Vol. 41, No. 5, Sept.–Oct. 2004.

[2] Woodstock, G., "Controllability of Large SEP for Earth Orbit Raising," 40th AIAA/ASME/SAE/ASEE Joint Propulsion Conference and Exhibit, Fort Lauderdale, FL, AIAA Paper 2004-3643, 2004.

[3] Kerslake, T. W., and Gefert, L. P., "Solar Power System Analyses for Electric Propulsion Missions," NASA TM-1999-209289, 1999; also Society of Automotive Engineers Paper 99-01-2449.

[4] Drake, B. G., ed., "Reference Mission Version 3.0 Addendum to the Human Exploration of Mars," NASA SP-6107-ADD EX13-98-036, 1998.

[5] Sackett, L. L., Malchow, H. L., and Edelbaum, T. N., "Solar Electric Geocentric Transfer with Attitude Constraints: Analysis," NASA CR-134927, Aug. 1975.

[6] Sackett, L. L., Malchow, H. L., and Edelbaum, T. N., "Solar Electric Geocentric Transfer with Attitude Constraints: Program Manual," NASA CR-134927, Aug. 1975.

[7] Kluever, C. A., and Oleson, S. R., "Direct Approach for Computing Near-Optimal Low-Thrust Earth-Orbit Transfers," *Journal of Spacecraft and Rockets*, Vol. 35, No. 4, July–Aug. 1998.

[8] Gill, P. E., Murray, W., Saunders, M. A., and Wright, M. H., "User's Guide for NPSOL (Version 4.0): A Fortran Package for Nonlinear Programming," Systems Optimization Lab., Stanford Univ., Stanford, CA, Jan. 1986.

[9] Choueiri, E. Y., “A Critical History of Electric Propulsion: The First 50 Years (1906–1956),” *Journal of Propulsion and Power*, Vol. 20, No. 2, Mar.–Apr. 2004.

[10] Oleson, S. R., “Mission Advantages of Constant Power, Variable I_{sp} Electrostatic Thrusters,” AIAA Paper 2000-3413, July 2000.

[11] Meissinger, H. F., Dawson, S., and Wertz, J. R., “A Low-Cost Modified Launch Mode for High C_3 Interplanetary Missions,” American Astronautical Society Paper 97-711, Sept. 1997.

[12] Wertz, J. R., and Larson, W. J., *Space Mission Analysis and Design*, 3rd ed., Microcosm, El Segundo, CA, 1999.

[13] Singh, S., “Xenon: A Modern Anaesthetic,” *Express Healthcare Management*, Indian Express Newspapers Ltd., Mumbai, India, May 2005.

[14] Vallado, D. A., *Fundamentals of Astrodynamics and Applications*, 2nd ed., Microcosm, El Segundo, CA, 2001.

[15] Wehrle, V. A., and Beaudette, S., “Earth Eclipse Evasion (E^3) Orbits,” *Canadian Aeronautics and Space Journal*, Vol. 49, No. 3, Sept. 2003.

J. Martin
Associate Editor